Comparison between linear FM and phase-coded CW radars

N. Levanon
B. Getz

Indexing terms: Linear FM radar, Phase-coded CW radar, Doppler compensation, Multicorrelation processor, Single correlator, Matched filters

Abstract: The classical linear FM CW radar signal is compared with P3 and P4 phase-coded CW signals. The comparison covers the theoretical delay–Doppler response, the spectrum and the performances in digital receiver processors. The receivers produce a matrix of delay and Doppler cells. Three receiver approaches are considered: (*a*) Doppler compensation followed by a multicorrelation processor. This is a general and efficient implementation of many matched filters, which applies to any phase-coded signal. (*b*) A modification of (*a*), applicable to P3, P4 signals, in which the multicorrelators are efficiently replaced by FFTs, without altering the performances. (*c*) A single correlator followed by two levels of spectral analysis, for range and for Doppler. In the two matched filter implementations, (*a*) and (*b*), the P signals exhibit lower range sidelobes, due to their inherent property of perfect periodic autocorrelation. The LFM signal requires additional weighting (hence additional SNR loss) and even then does not approach the low range sidelobes of P signals. In the single correlator receiver, the two signals exhibit almost identical performances, which are similar to the performances of LFM in the matched receiver.

1 Introduction

Frequency modulated continuous wave (FMCW) radars enjoy renewed interest [1, 2]. This interest is attributed in part to the need for low probability of intercept (LPI) by conventional electronic support measures (ESM) which are matched to pulse radars [3]. At the same time there has been a surge of new phase-coded signals, especially appealing to CW radars because of their perfect periodic autocorrelation. Prominent among them are the Lewis and Kretschmer P3 and P4 polyphase signals [4] which are closely related to linear FM (LFM) signals. Biphase signals can also exhibit perfect periodic autocorrelation (zero sidelobes), as indicated independently by Bomer [5] and Golomb [6]. Finally, there are binary signals (i.e. biphase utilising 0° and 180°), suggested by Ipatov and Fedorov [7], which exhibit low loss, zero sidelobes, crosscorrelation with a slightly mismatched reference signal.

The LFM signal does not exhibit perfect periodic autocorrelation and must suffer from some level of range sidelobes. On the other hand it has three practical advantages: (i) LFM utilises the spectrum efficiently, with no frequency sidelobes; (ii) linear frequency modulation is considered easier to implement than phase coded modulation (at least, as long as there is no strict demand on linearity specifications over a wide bandwidth); (iii) linear FM can be processed using one multiplication with a matched reference signal. The range can then be resolved using spectral analysis of the product. While this is not a matched receiver, its performance, at least over a limited delay span, is close to the performance of a matched receiver. Of the phase coded signals, only P3 and P4 exhibit a similar property and can utilise simpler processing. The other phase coded signals exhibit their ideal range response only when processed by a matched receiver, which implies a separate correlation for each range cell of interest.

In the following Sections we will compare the performance of a P3 (or P4) signal with the corresponding LFM signal, using both matched (many correlators) and simplified (single correlator) receivers for both type of signals. Weight functions will be utilised in the time domain to reduce the Doppler sidelobes. In the case of LFM, weighting in the frequency domain will be added to reduce range sidelobes. Digital signal processing requires sampling of the received signal. In the phase-coded signal there is an obvious sampling choice: one sample per bit. LFM will require more attention to this issue.

If we wish to maintain equal range resolution by both signals, the frequency deviation, Δf, of the LFM will have to be equal to the inverse of the bit duration, t_b, of the P signals,

$$\Delta f = \frac{1}{t_b} \tag{1}$$

The range resolution of both signals is now

$$\Delta R = \frac{C}{2\,\Delta f} = \frac{Ct_b}{2} \tag{2}$$

Also, eqn. 1 implies that the two signals will occupy a similar effective bandwidth. The power spectrum of LFM is nearly rectangular over the band $f_c - \Delta f/2 < f < f_c + \Delta f/2$. The power spectrum of P signals is relative to $\mathrm{sinc}^2[(f - f_c)t_b]$. Thus both spectrums have their 3 dB points near $f = f_c \pm \Delta f/2 = f_c \pm 1/(2t_b)$. (See Appendix 11.3.)

If both signals will have the same modulation period

Paper 1233F (E15, E5), first received 16th March 1993 and in revised form 14th February 1994

The authors are with the Department of Electrical Engineering-Systems, Tel-Aviv University, Tel-Aviv, Israel

T, then the sequence length M (the number of bits within one modulation period of the phase-coded signal) is given by

$$M = \frac{T}{t_b} \tag{3}$$

From eqns. 1 and 3 we find that with these conditions

$$M = T\,\Delta f \tag{4}$$

which means that the 'sequence length' of the phase-coded signal is the equivalent of the 'time–bandwidth product' of the LFM. Both are also called the 'processing gain'.

2 Matched and mismatched receivers for periodic signals

A well known concept, in receiver design for finite duration signals, is the 'matched receiver' [8]. It performs correlation between the received signal and a reference signal whose envelope is the complex conjugate of the envelope of the transmitted signal. Since the received signal is usually delayed and Doppler shifted, there is a special interest in the response of a matched receiver (to its own signal) as a function of the two parameters, delay and Doppler. This response is called the 'ambiguity function'.

Consider now a periodically modulated CW signal, whose complex envelope $u(t)$ obeys

$$u(t) = u(t - nT) \quad n = 0, \pm 1, \pm 2, \ldots \tag{5}$$

The receiver can obviously match only a finite section of the transmitted signal. For convenience let us assume that the length of that section is an integer multiple N of the modulation period T. Let us also assume that the target illumination time (dwell time) is PT and that PT is longer than NT. As long as the delay τ is shorter than the difference between the dwell time and the length of the reference signal, the illumination time can be considered infinitely long and the receiver response can be described by a 'periodic ambiguity function' (PAF),

$$|\chi_{NT}(\tau, v)| = \left| \int_0^{NT} u(t - \tau)u^*(t) \exp(j2\pi vt)\, dt \right| \tag{6}$$

where τ is assumed a constant, and its change with time is expressed in the Doppler shift v. Because τ is considered a constant, $u(t - \tau)$ has the same period length as $u(t)$ and $u^*(t)$, as given in eqn. 5. If we define a rectangular window function

$$p(t) = \begin{cases} 1 & 0 \leqslant t \leqslant NT \\ 0 & \text{elsewhere} \end{cases} \tag{7}$$

then eqn. 6 could also be written as

$$|\chi_{NT}(\tau, v)| = \left| \int_{-\infty}^{\infty} u(t - \tau)u^*(t)p(t) \exp(j2\pi vt)\, dt \right| \tag{8}$$

Increasing N improves the Doppler resolution. As pointed out in Reference 9, no matter what $u(t)$ is, the PAF obeys a universal relationship

$$|\chi_{NT}(\tau, v)| = |\chi_T(\tau, v)| \left| \frac{\sin(N\pi vT)}{N \sin(\pi vT)} \right| \tag{9}$$

which means that for large N the PAF is increasingly attenuated for all values of the Doppler shift v, except at multiples of $1/T$. The nature of the $|\sin(Nx)/N \sin(x)|$ term is that in addition to the main lobes at $x = n\pi$, $n = 0, \pm 1, \pm 2, \ldots$, it also has relatively strong sidelobes. These will appear as Doppler sidelobes of the PAF. To reduce the Doppler sidelobes it is necessary to modify the reference signal. A modified reference signal converts the receiver from a matched receiver to a mismatched one, with its associated effect of a loss in the output signal-to-noise ratio (SNR).

For future use let us divide the new reference signal to a product of two signals $r(t)$ and $w(t)$. $r(t)$ will be periodic, with the same period as $u(t)$. $w(t)$ will be an aperiodic weight function. Both functions are still multiplied by the rectangular window $p(t)$ defined in eqn. 7. The delay–Doppler response of the mismatched receiver will be

$$|\varphi(\tau, v)| = \left| \int_{-\infty}^{\infty} u(t - \tau)r(t)p(t)w(t) \exp(j2\pi vt)\, dt \right| \tag{10}$$

Except for a missing negative sign in the exponent, eqn. 10 is effectively the Fourier transform of two products $u(t - \tau)r(t)$ and $p(t)w(t)$. It can therefore be described by convolution on the v axis (denoted by $\otimes$) of two Fourier transforms,

$$|\varphi(\tau, v)| = \left| \int_{-\infty}^{\infty} u(t - \tau)r(t) \exp(j2\pi vt)\, dt \otimes \int_{-\infty}^{\infty} p(t)w(t) \exp(j2\pi vt)\, dt \right| \tag{11}$$

The first integral in eqn. 11 is the Fourier transform of $u(t - \tau)r(t)$. Since $u(t)$ and $r(t)$ are both periodic with the same period T, the Fourier transform of their product (for any τ) will be a series of impulses,

$$\int_{-\infty}^{\infty} u(t - \tau)r(t) \exp(j2\pi vt)\, dt = \sum_{n=-\infty}^{\infty} \delta\left(v - \frac{n}{T}\right) g_n(\tau) \tag{12}$$

where

$$g_n(\tau) \triangleq \frac{1}{T} \int_0^T u(t - \tau)r(t) \exp\frac{j2\pi nt}{T}\, dt \tag{13}$$

The second integral in eqn. 11 is the transform of the weight function extended over the duration of the rectangular window $p(t)$. It will be termed $W(v)$,

$$W(v) = \int_{-\infty}^{\infty} p(t)w(t) \exp(j2\pi vt)\, dt = \int_0^{NT} w(t) \exp(j2\pi vt)\, dt \tag{14}$$

The delay–Doppler response of the weighted correlation receiver is obtained from the convolution between eqns. 12 and 14, yielding

$$|\varphi(\tau, v)| = \left| \sum_{n=-\infty}^{\infty} W\left(v - \frac{n}{T}\right) g_n(\tau) \right| \tag{15}$$

The meaning of eqn. 15 is that at any given delay–Doppler coordinate (τ, v) the receiver response is determined by contributions from all the g_n functions, for that value of τ. Each g_n contributes according to the value of $W(\hat{v} - n/T)|_{\hat{v}=v}$. The behaviour of $W(v)$ will be determined by the weight function. The set of functions $g_n(\tau)$ will be determined by the transmitted signal and by the reference signal.

3 Weight functions

$w(t)$ is the weight function across the entire duration of the reference signal. Selecting the parameter c in the fol-

lowing expression will determine three simple yet important '2-term' weight windows,

$$p(t)w(t) = \frac{1}{NT}\left(1 - \frac{1-c}{c}\cos\frac{2\pi t}{NT}\right)$$
$$0 \leqslant t \leqslant NT \quad \text{zero elsewhere} \quad (16)$$

For uniform, Hann and Hamming weight windows, $c = 1$, 0.5 and 0.53836, respectively. Applying the transform in eqn. 14, we get

$$W(v) = \frac{\sin(\pi vNT)}{\pi vNT}\left(1 + \frac{(1-c)(vNT)^2}{c[1-(vNT)^2]}\right) \times \exp(j\pi vNT) \quad (17)$$

When $(vNT)^2 = 1$ eqn. 17 yields $W(v) = -(1-c)/(2c)$. Note also that exactly at multiples of n/T, $n \neq 0$, the function $W(v)$, as defined in eqn. 17, becomes zero, i.e.

$$W(n/T) = 0 \quad n = \pm 1, \pm 2, \ldots \quad (18)$$

For Hann, and $N = 16$, the fall-off rate determines that the contribution of say $g_1(\tau)$ on the response near $v = 0$ (more exactly at $v = 1/2NT$) is attenuated by about 82 dB compared to the contribution of $g_0(\tau)$ at $v = 0$.

4 Linear FM

In this Section we will present the function $g_n(\tau)$ for a linear FM (LFM) signal and a receiver in which the envelope of the reference signal (before adding weights) is the complex conjugate of the envelope of the transmitted signal,

$$r(t) = u^*(t) \quad (19)$$

The LFM signal in our example will have its frequency as a sum of the fixed carrier frequency, f_c, and a periodic function:

$$\left.\begin{aligned} f(t) &= \sum_n f_T(t - nT) \quad n = 0, \pm 1, \pm 2, \ldots \\ f_T(t) &= f_c + \frac{\Delta f}{T}\left(t - \frac{T}{2}\right) \\ &\qquad 0 \leqslant t \leqslant T \quad \text{zero elsewhere} \end{aligned}\right\} \quad (20)$$

which implies that the complex envelope of the transmitted signal is

$$\left.\begin{aligned} u(t) &= \sum_n u_T(t - nT) \quad n = 0, \pm 1, \pm 2, \ldots \\ u_T(t) &= \exp\frac{j\pi\,\Delta f\left(t - \frac{T}{2}\right)^2}{T} \\ &\qquad 0 \leqslant t \leqslant T \quad \text{zero elsewhere} \end{aligned}\right\} \quad (21)$$

Using eqns. 21 and 19 in eqn. 13 yields

$$g_n(\tau) = \left[\frac{\tau}{T}\frac{\sin\alpha}{\alpha} + (-1)^n\left(1 - \frac{\tau}{T}\right)\frac{\sin(\pi n - \alpha)}{\pi n - \alpha}\right] \times \exp\left(\frac{j\pi n\tau}{T}\right) \quad (22)$$

where

$$\alpha = \frac{\pi\tau}{T}[\Delta f(T - \tau) + n] \quad (23)$$

A linear-scale plot of $|g_n(\tau)|$, $n = -2$ to 24, $0 \leqslant \tau \leqslant T$, is given in Fig. 1, for an LFM signal with $T\,\Delta f = 20$.

Let us study more carefully the zero Doppler ridge $g_0(\tau)$. Setting $n = 0$ in eqn. 22 yields

$$g_0(\tau) = \frac{\sin\alpha}{\alpha} \quad \alpha = \pi\tau\,\Delta f\left(1 - \frac{\tau}{T}\right) \quad (24)$$

Furthermore, for small delay

$$g_0(\tau) \approx \frac{\sin(\pi\tau\,\Delta f)}{\pi\tau\,\Delta f} \quad \tau \ll T \quad (25)$$

The first null (zero value) of eqn. 25 occurs when the argument is equal to π, namely when $\tau = 1/\Delta f$. Hence the common notion that the delay resolution of a linear FM signal is the inverse of the frequency deviation. As to higher order ridges, note that as long as $\tau \ll T$, eqn. 22 could be simplified to

$$|g_n(\tau)| \approx \left|\frac{\sin(\pi\tau\,\Delta f)}{\pi(n - \tau\,\Delta f)}\right| \quad \tau \ll T \quad (26)$$

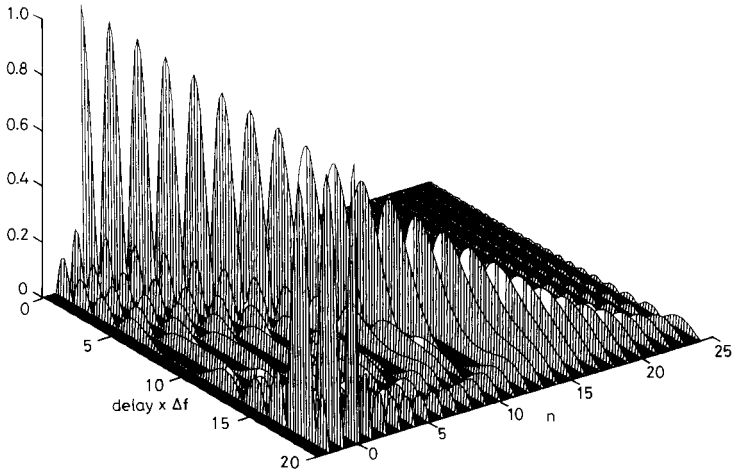

Fig. 1 $|g_n(\tau)|$ *of an LFM signal with* $T\,\Delta f = 20$, *for* $n = -2$ *to* 24
Linear voltage scale
$(0 \leqslant \tau \leqslant T)$

which peaks at $\tau = n/\Delta f$. The properties of $|g_n(\tau)|$ for small delay, as expressed in eqns. 25 and 26 are demonstrated in Fig. 2. This is an expanded section of $|g_n(\tau)|$ for $n = -1$ to 4 and for $0 \leqslant \tau \leqslant 8/\Delta f$, for an LFM signal with $T\,\Delta f = 10^4$.

Figs. 1 and 2 demonstrate the extensive range sidelobes of $|g_n(\tau)|$ which will appear also in the receiver delay–Doppler response $|\varphi(\tau, \nu)|$. As a matter of fact $|g_n(\tau)|$ represents $|\varphi(\tau, n/T)|$ for very large N. This is because for very large N the weighted receiver response contains mainly ridges at $\nu = n/T$, while the Doppler sidelobes between them are rapidly suppressed due to the rapid decay of $W(\nu)$. Hence, the ridges are practically identical to their corresponding $|g_n(\tau)|$.

The overall weight function suppresses *Doppler* sidelobes. To reduce *range* sidelobes we will adopt the well known practice of frequency weighting, used in LFM pulse compression (Section 7.2 of Reference 8). Since the entire frequency deviation is linearly swept within one modulation period T, frequency weighting can be implemented by a repetitive time weight function with a period T. More specifically

$$r(t) = \sum_n r_T(t - nT) \quad n = 0, \pm 1, \pm 2, \ldots \tag{27}$$

where

$$r_T(t) = u_T^*(t) w_T(t) \tag{28}$$

To stay with the simple '2-term' type of weight function discussed before, let

$$w_T(t) = 1 - \frac{1-c}{c} \cos \frac{2\pi t}{T}$$

$$0 \leqslant t \leqslant T \quad \text{zero elsewhere} \tag{29}$$

With this particular internal weight function, the $g_n(\tau)$ function will now be designated $g_{nw}(\tau)$ and it can easily be shown that

$$g_{nw}(\tau) = g_n(\tau) - \frac{1-c}{2c} [g_{n+1}(\tau) + g_{n-1}(\tau)] \tag{30}$$

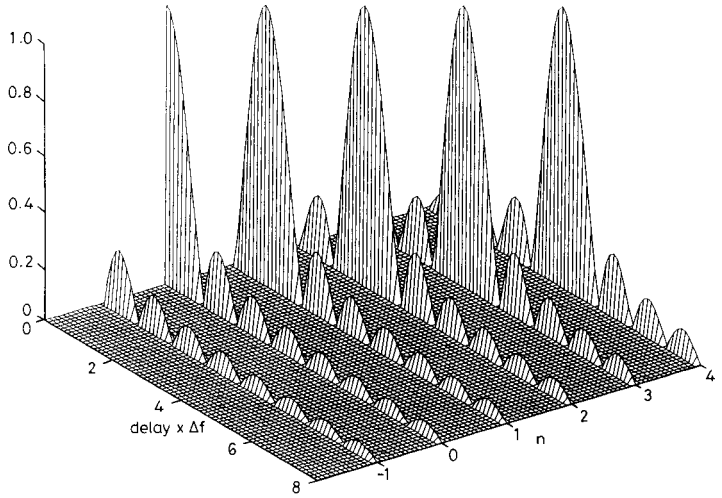

Fig. 2 *$|g_n(\tau)|$ of an LFM signal with $T\,\Delta f = 10^4$, for $n = -1$ to 4*
($0 \leqslant \tau \leqslant 8/\Delta f$)

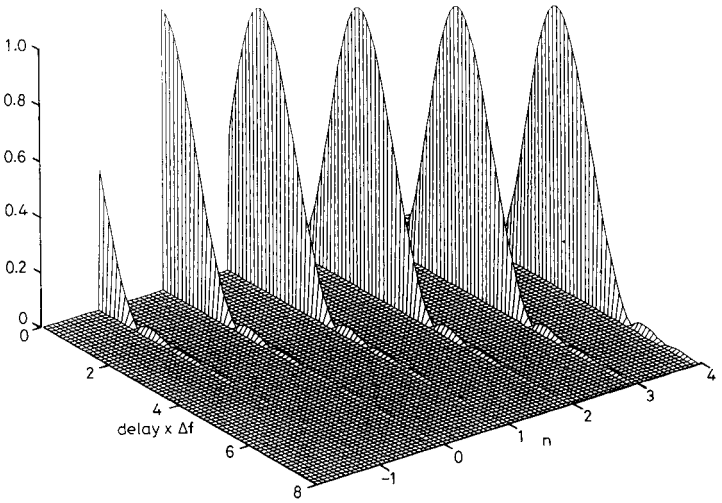

Fig. 3 *The effect of Hann weighting on Fig. 2*

Note that the designation $g_n(\tau)$ is reserved for the case of a *uniform* internal weight function.

Fig. 3 is a plot of $|g_{nw}(\tau)|$ for Hann internal weight function, and otherwise the same parameters as in Fig. 2. With Hann weighting the peak sidelobe (PSL) of $|g_{0w}(\tau)|$ drops to -31.5 dB, but the mainlobe is wider, with a first null at $\tau = 2/\Delta f$. Further reduction of range sidelobes can be achieved with a more complex internal weight function, at the expense of a wider mainlobe. The 'minimum' 4-term window [10] exhibits a PSL of -92 dB, but the first null is at $\tau = 4/\Delta f$.

Plots of $|\varphi(\tau, \nu)|$ for an LFM signal with $T\,\Delta f = 10^4$ are given in Figs. 4 and 5. Fig. 4 applies to a Hann internal weight, while Fig. 5 applies to the 'minimum' 4-term internal weight. The vertical scale is logarithmic, with a floor at -140 dB. In both cases $T\,\Delta f = 10^4$ and $N = 16$. The delay and Doppler scales are: $0 \leqslant \tau \leqslant 10/\Delta f$ and $-2/NT \leqslant \nu \leqslant 1/T + 2/NT$, which means that the Doppler axis extends slightly beyond the first ambiguous Doppler ridge at $\nu = 1/T$. In both figures the *aperiodic* weight function is Hann. An *aperiodic* weight function with more terms would lower the Doppler sidelobe (between the ridges) but would increase the width of the ridges along the Doppler axis. Increasing N would lower the contribution of the sidelobes of one ridge on its neighbours. However, the range sidelobes on the delay axis, could not be reduced below the sidelobes of $|g_{0w}(\tau)|$. More complicated *periodic* (internal) weight

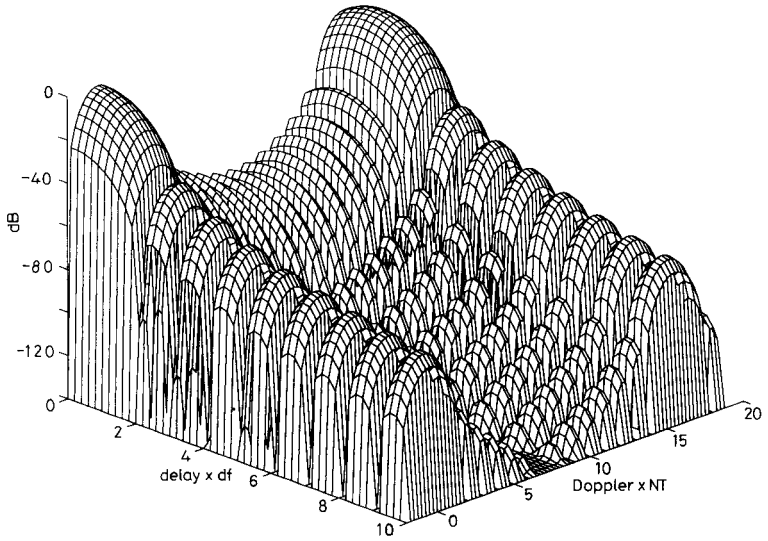

Fig. 4 *Log display (floor at -140 dB) of the theoretical response of a receiver matched to $N = 16$ periods of an LFM signal with $T\,\Delta f = 10^4$*
Hann Doppler and delay weighting
($0 \leqslant \tau \leqslant 10/\Delta f$, $-2/NT \leqslant \nu \leqslant 1/T + 2/NT$)

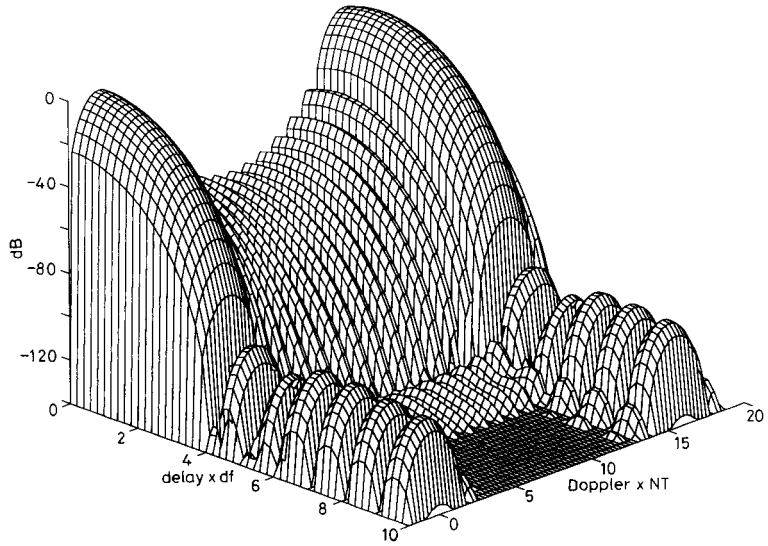

Fig. 5 *Log display (floor at -140 dB) of the theoretical response of a receiver matched to $N = 16$ periods of an LFM signal with $T\,\Delta f = 10^4$*
Hann Doppler and 'minimum' 4-term delay weighting
($0 \leqslant \tau \leqslant 10/\Delta f$, $-2/NT \leqslant \nu \leqslant 1/T + 2/NT$)

windows could further lower these range sidelobes, at the expense of further widening the main range lobe. However, drastic reduction of range sidelobes without widening the main range lobe, could not be achieved with an LFM signal. It can, however, be achieved with a phase-coded signal, as discussed in the following Section.

5 Phase-coded CW periodically-modulated signals

In phase-coded CW periodically-modulated signals the period of the modulation signal is divided into M bits, each of duration t_b

$$T = Mt_b \tag{31}$$

with

$$u_T(t) = \sum_{m=1}^{M} u_m[t - (m-1)t_b] \qquad 0 \leqslant t \leqslant T \quad \text{zero elsewhere} \tag{32}$$

The bits are phase modulated by the phase sequence $\{\phi_m\}$ of length M,

$$u_m(t) = \begin{cases} \exp(j\phi_m) & 0 \leqslant t \leqslant t_b \\ 0 & \text{elsewhere} \end{cases} \tag{33}$$

For such a phase coded signal and when $r(t) = u^*(t)$, the function $g_n(\tau)$ is given by

$$\begin{aligned} g_n(\tau_0 + pt_b) &= \frac{1}{M}\sum_{m=1}^{M} \exp\left[j2\pi(m-1)\frac{n}{M}\right]\left\{\frac{\tau_0}{t_b}\frac{\sin(\pi n\tau_0/T)}{(\pi n\tau_0/T)}\right. \\ &\quad \times \exp\left[j(\phi_{M+m-p-1} - \phi_m + (\pi n\tau_0/T))\right] \\ &\quad + \left(1 - \frac{\tau_0}{t_b}\right)\frac{\sin(\pi n(t_b - \tau_0)/T)}{\pi n(t_b - \tau_0)/T} \\ &\quad \left. \times \exp\left[j\left(\phi_{M+m-p} - \phi_m + \frac{\pi n(t_b + \tau_0)}{T}\right)\right]\right\} \end{aligned} \tag{34}$$

where $0 \leqslant \tau_0 < t_b$ and $p = 0, 1, 2, \ldots$. Note that a negative delay can be described by its complement to T, since

$$g_n(-\tau) = g_n(T - \tau) \tag{35}$$

Eqn. 34 applies to any sequence of phase coding. In the following Section it will be used to study the P3 and P4 signals.

6 P3 and P4 polyphase codes

These codes, suggested by Lewis and Kretschmer [4], are basically phase samples of a linear FM signal. The phase sequence of a P4 signal can be described by

$$\phi_m = \frac{\pi}{M}(m-1)^2 - \pi(m-1) \quad m = 1, 2, \ldots, M \tag{36}$$

and of the P3 signal (first suggested by Chu [11]) by

$$\phi_m = \frac{\pi}{M}(m-1)^2 \quad m = 1, 2, \ldots, M \quad M \text{ even} \tag{37}$$

In addition to the property of perfect periodic autocorrelation, these signals exhibit a unique feature. When a phase staircase is added, with a stair width t_b, and it results in a phase accumulation of 2π over one sequence, the new code is a one bit shift of the original code (plus a constant phase). Using eqn. 36 note for P4 that

$$\phi_m + \frac{2\pi}{M}(m-1) = \phi_{m+1} + \pi\left(1 - \frac{1}{M}\right) \tag{38}$$

A similar result is obtained for a P3 signal.

Cross-correlation between a conjugate of the original signal and the signal with the added phase staircase, will result in a one bit shift of the perfect periodic autocorrelation. A phase staircase which accumulates $2\pi n$ phase shift over one sequence will result a shift of n bits of the autocorrelation function.

Doppler shift creates a 'phase ramp' rather than a 'phase staircase'. The ramp means that there is also a linear phase shift within each bit. For $v = n/T$ the result is still a sidelobe-free, n-bit shifted autocorreation. However, as n increases, the phase shift within each bit begins to modify the ideal triangular form of the cross-correlation. This is demonstrated in Fig. 6 which is a plot of $|g_n(\tau)|$ for $n = -2, -1, 0, 1, \ldots, M-1$. Fig. 6 applies to a P4 signal with $M = 16$. Fig. 6 falsely hints of an intrabit symmetry, because it shows that

$$|g_n(nt_b + \tau_0)| = |g_n(nt_b - \tau_0)| \quad |\tau_0| < t_b \tag{39}$$

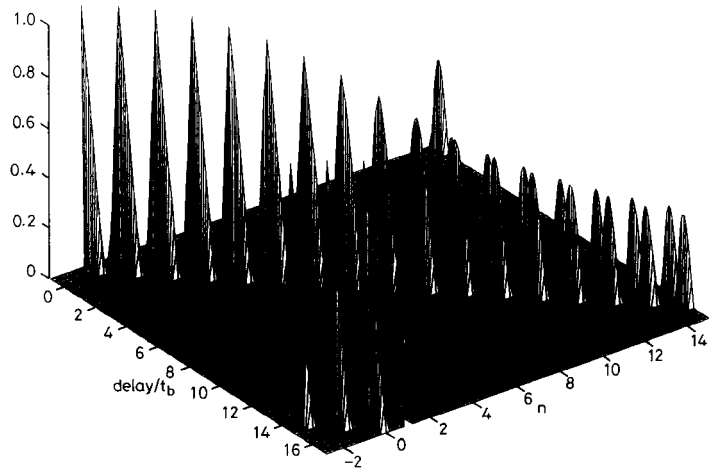

Fig. 6 *$|g_n(\tau)|$ of a P4 signal with $M = 16$, for $n = -2$ to $M - 1$*
Linear voltage scale
$(-t_b \leqslant \tau \leqslant T + t_b)$

The symmetry, however, holds only for the absolute value and not for $g_n(\tau)$ itself.

One conclusion from the unique property of $g_n(\tau)$ for P3 and P4 signals is that, for eqn. 15 to properly describe the response, it is necessary to extend the sum in eqn. 15 to $|n| > M/2$. For example, at $\tau = T/2$ the receiver response, even near $\nu = 0$, is controlled by the two ridges corresponding to $n = \pm M/2$. There are no closer ridges that contribute an effect which will overshadow the effect of those two distant ridges.

Fig. 7 is a 3D plot of the response (as given in eqn. 15) of a Hann weighted receiver to a P4 signal with $M = 24$, $N = 16$. The vertical scale is logarithmic with a floor at -140 dB. The delay axis extends over $0 \leqslant \tau \leqslant 10t_b$. The Doppler axis extends over $-2/NT \leqslant \nu \leqslant 1/T + 3/NT$. Note that the sidelobe structure near $\tau = 0$ is not affected by M. Recall the lack of effect of the time–bandwidth product on the sidelobe structure of an LFM signal near zero delay. Fig. 7 should be compared to Figs. 4 and 5 which describe a similar section of the response for an LFM signal. The comparison demonstrates clearly the considerably lower sidelobes of the P4 signal. A P3 signal would have yielded a response very similar to that of a P4 signal.

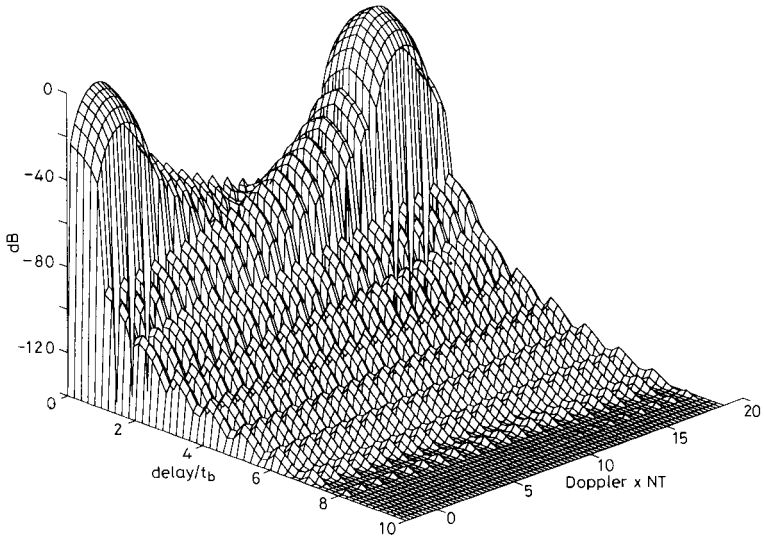

Fig. 7 *Log display (floor at −140 dB) of the theoretical response of a receiver matched to N = 16 periods of a P4 signal with M = 24*
Hann Doppler weighting
$(0 \leqslant \tau \leqslant 10t_b, -2/NT \leqslant \nu \leqslant 1/T + 3/NT)$

Owing to the perfect periodic autocorrelation property, there are no delay sidelobes exactly on $\nu = 0$. The delay sidelobes near $\nu = 0$ are caused by contribution from $g_n(\tau)$, $n \neq 0$, namely, by the sidelobe flow from the neighbouring ridges. This effect can be reduced by increasing N. Another approach is to use more terms in the weight function. This will decrease the Doppler sidelobes at a cost of widening each ridge width in the Doppler axis.

The conclusion from the above comparison is that if a matched filter is implemented in the receiver, then a P4 (or P3) signal should be preferred to a linear FM signal. How should that be compared with the relative ease of generating LFM signals? As a matter of fact the difference is questionable. To generate high quality LFM signals, digital generation is required [12]. Digital generation as described in Reference 12 is through phase steps. To maintain the delay resolution of $1/\Delta f$, the step duration should not exceed the delay resolution. Thus we come back to a phase coded signal with $t_b = 1/\Delta f$ and a sequence length of $M = T\,\Delta f$ bits. Then, if the phase follows the quadratic law typical of LFM, a P4 (or P3) signal will result.

P signals have an advantage over LFM also from the point of view of SNR loss. Recall that LFM required an additional periodic weight function to suppress delay sidelobes. An analysis of the SNR loss is given in Appendix 11.1.

7 Matched-filter implementations

So far we have discussed the theoretical periodic ambiguity function (including weighting). In this Section we will suggest an implementation of $M \times N$ matched filters. The MN outputs of these filters, when the input is the signal at zero delay and Doppler shift, should be identical to the ambiguity function (more precisely to $M \times N$ samples of it). For any other choice of delay and Doppler, the function will be shifted accordingly.

A true matched receiver involves a correlator for each range cell. In other words, a receiver matched to a phase-coded signal delayed by kt_b, requires correlation with the M-bit conjugate sequence, after a cyclic shift of k bits. To cover more velocity cells than the zero Doppler cell, it is necessary to introduce phase compensation to the phase ramp generated by the Doppler frequency shift. A convenient way to implement simultaneously several phase ramps is through an FFT processor.

A relatively efficient implementation of a processor, that constitutes several matched filters, is presented in Fig. 8A. The processor is matched to N sequences, of an M bit code. Digital samples of the complex envelope of the received signal (obtained with I & Q sampling) are stored in a register of length MN. The MN complex samples are first multiplied by the MN values of the weight function. Coarse Doppler compensation is obtained in the next stage which performs M FFTs, each

one with N inputs. FFT1 operates on the first (weighted) bit of each one of the N sequences. FFT2 on the second bit, etc. Fine Doppler compensation is performed in the

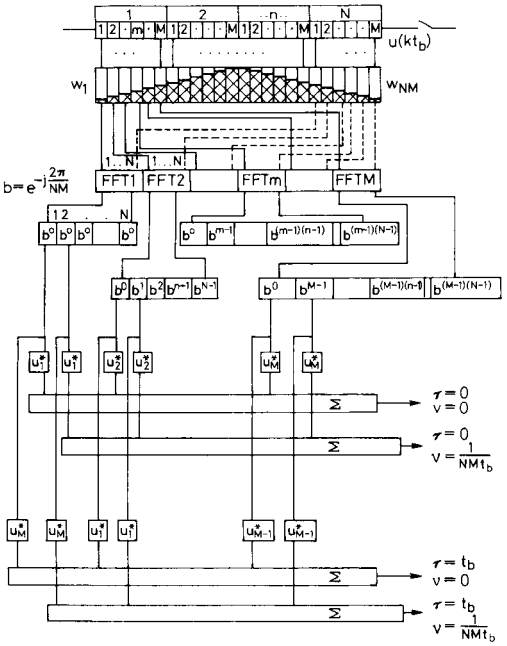

Fig. 8A *Implementation of a multicorrelator receiver*

complex matrix (with elements b^n) that multiplies all the FFT outputs. Next, we obtain a set of NM correlators. The top correlator operates on the zero Doppler output of each one of the M FFTs, and multiplies them by an unshifted conjugate of the transmitted sequence. The adder output corresponds to the $\tau = 0$, $v = 0$ cell. In the second correlator from the top, an identical unshifted reference multiplies the second output of all the FFTs. Its output corresponds to the $\tau = 0$, $v = 1/NMt_b$ cell. The total number of correlators for the $\tau = 0$ cell is N, but only two are plotted. The lower pair of correlators in the illustration correspond to the first two Doppler cells of the $\tau = t_b$ delay. It involves a reference signal with a cyclic shift of one bit. Again, N correlators are needed in connection with that delay in order to cover all the Doppler shifts over a Doppler band of $1/T(=1/Mt_b)$.

Although the FFTs compensate for the Doppler phase shift between consecutive *sequences*, the complex matrix (with elements b^n), which multiplies the outputs of the FFTs, is responsible for compensating the phase shift between consecutive *bits*. Note that for the Doppler step $\Delta v = 1/NMt_b$ the corresponding phase shift over the duration of one bit t_b is

$$\Delta\phi = 2\pi\,\Delta v t_b = \frac{2\pi}{NM} \tag{40}$$

In Fig. 8A, the matrix of elements $b^n = \exp(-jn\,\Delta\phi)$, $n = 1, 2, \ldots, (M-1)(N-1)$, compensates that phase shift. The phase shift (for the first Doppler) between consecutive sequences is $\Delta\Phi = M\,\Delta\phi = 2\pi/N$, and it is compensated by the FFTs.

The number of multiplications required by the processor in Fig. 8A, to cover all the MN unambiguous elements in the delay–Doppler matrix of the response, is given by $M[NM + 2N + N\log_2(N)]$. For comparison, a brute force processor involves M repeats of a correlation and, for each repeat, an FFT on a vector of length NM. The number of multiplications required for such a processor is $M[NM + N + NM\log_2(NM)]$. This processor yields NM Doppler bins for each one of M range bins, and hence covers a larger Doppler band, of width M/T, which is mostly *ambiguous*. For the case $M = 64$, $N = 16$ the efficient processor requires about one tenth the number of multiplications required by the brute force processor.

It should be pointed out that the two processors suggested above are true banks of matched processors. The one described by Fig. 8A contains $M \times N$ cells (M delay and N Doppler) and the brute force one contains $M \times MN$ cells (M delay and MN Doppler). It will be a mistake to borrow processors used in pulse compression radars, which involve M correlations of length M, repeated for each modulation period, giving MN correlations, then M FFTs of length N to extract the Doppler information. This approach does not account for the Doppler-caused phase changes within each sequence of M bits. In pulse compression, where $Mt_b \ll T$, this could be allowed. However, in the CW case $Mt_b = T$, and the Doppler effect within the sequence could not be neglected and should be compensated by the matched filter.

The processor described in Fig. 8A was simulated in software and applied to P signals and to LFM signals. The LFM signals were simulated as phase-coded signals with quadratic phase law, and the only difference was that they did not achieve, during one period, a total phase shift of $M\pi$, as does a P3 signal. The simulation for the P3, P4 signals resulted a response identical to the theoretical one as given in Fig. 7, while the simulation for LFM (using the Hann internal weight) resulted a response similar to the one given in Fig. 4.

7.1 Implementing multicorrelation of P signals with FFTs

The $M \times N$ correlators (each one of length M) constitute most of the computational load of the processor in Fig. 8A. Fortunately, P3 and P4 signals with one sample per bit can be correlated using FFTs. As pointed out in eqn. 38, adding to the code a phase staircase with a step height of $2\pi n/M$, shifts the code by n bits. An FFT of length M implements M such staircases, each one with a different step height ($n = 0, 1, \ldots, M-1$). Thus the multicorrelators in Fig. 8A could be replaced by one multiplication with the conjugate of the code, followed by N FFTs, each one of length M (Fig. 8B).

Computer simulations of processing a P3 signal with the processor of Fig. 8B yielded exactly the same ideal performances as the processor of Fig. 8A. For a signal with code length $M = 128$, and $N = 16$ sequences, the processing was speeded up remarkably by a factor of 20.

The efficient processor of Fig. 8B can be applied also to an LFM signal approximated by quadratic phase coding. The output will again be exactly the same non-ideal response obtained with LFM in the processor of Fig. 8A.

From Fig. 8B we note two levels of FFTs: the first takes care of Doppler compensation and the second performs correlations. The property of LFM and P codes which allows this, also allows less ideal processing, which has been used extensively, and is described in the following Section. There, the role of the two FFT levels is reversed. The resulting processor is not a bank of

matched filters, and for P signals this causes loosing the ideal zero range sidelobes.

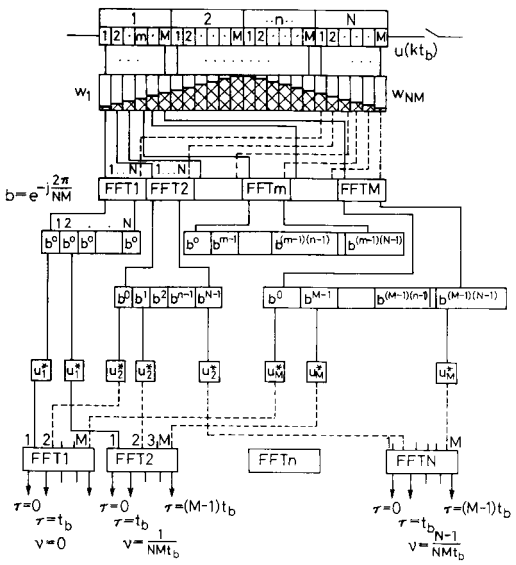

Fig. 8B *Efficient implementation of a multicorrelator receiver for P3 and P4 signals*

8 Single correlator processing of LFM

This kind of processing is unique to signals of the linear FM family. It stems from the fact that in LFM the instantaneous frequency difference between the transmitted signal and the delayed and Dopper-shifted received signal is a periodic two-valued function, depicted in Fig. 9. For small delay ($\tau \ll T$), the dominant beat frequency is the 'lower beat note' [13]

$$f_{bl} = \Delta f \frac{\tau}{T} - f_D \tag{41}$$

which is linearly related to the delay, τ, with a bias due to the Doppler shift. It is interesting to note that the number of cycles of the lower beat frequency (without Doppler), within one modulation period, is $Tf_{bl} = \tau \Delta f$.

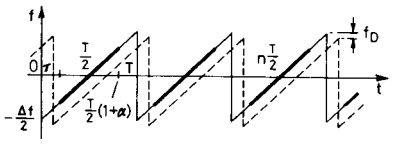

Fig. 9A *Frequency of the transmitted and reflected LFM signal*

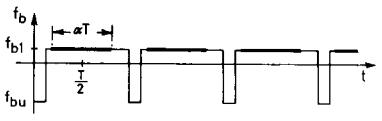

Fig. 9B *Beat frequency*

When the coherent processing time extends over several modulation periods, the spectrum of the beat signal is constructed of spectral lines [13] at intervals of $1/T$, whose envelope peaks near the value of the instantaneous beat frequency given in eqn. 41 and also around the complement value to Δf, the 'upper beat note', namely

$$f_{bu} = \Delta f\left(1 - \frac{\tau}{T}\right) + f_D \tag{42}$$

Many LFM CW radars utilise this property, and perform spectral analysis of the beat signal. The spectral analysis can be implemented in different ways, e.g. a bank of filters or an FFT.

It is possible to avoid the upper beat frequency by limiting the processing of the beat signal to sections in which only the lower beat frequency exists. An example would be the emphasised sections in Fig. 9. When the radar operates within the condition $\tau \ll T$, the upper beat note is usually high enough to be well outside the receiver bandpass, and is not a problem. Even then it is good practice to avoid the vicinity of the modulation transient (the 'fly back'). Hence, within each period T of the reference signal, the processed section is of duration αT (with $0 < \alpha < 1$), and it is centred about $T/2$. As long as the delay τ is limited to the range

$$|\tau| \leqslant \tau_{max} = (1 - \alpha)\frac{T}{2} \quad 0 < \alpha < 1 \tag{43}$$

only the lower beat frequency will exist.

If several sections are processed coherently, e.g. by FFTs, then further Doppler processing can be performed on outputs corresponding to the same range gate. The different sections can each be in a different modulation period, or within the same modulation period. The following discussion assumes different modulation periods.

A concise block diagram of such a processor appeared in Fig. 2 of Reference 2. We present a more detailed diagram in Fig. 10. N complete modulation periods of

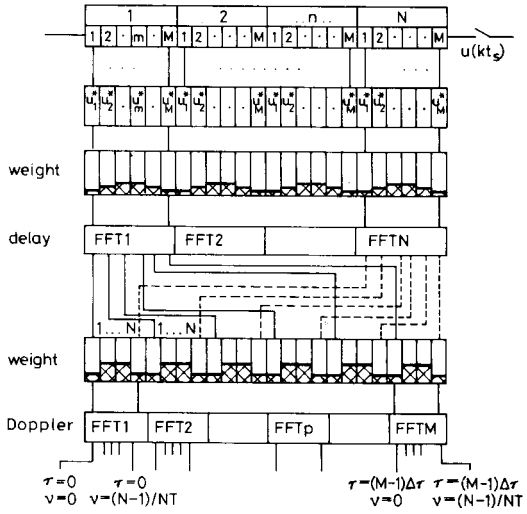

Fig. 10 *A single correlator receiver for LFM and P signals*

the complex envelope of the received signal, sampled at intervals of t_s, are stored in a register of length NM. They are multiplied by a reference signal, which is the complex conjugate of the same N periods. In linear FM we use only K *consecutive* samples out of the M samples in each period. In P signals we use all the M samples. In the first FFT level, a Fourier transform is performed on *one* modulation period, or part of it. The transform is repeated N times, covering N modulation periods. The pth

output of each FFT corresponds to the pth range gate. In the second FFT level, the transform is performed on the pth output of each one of the N FFTs. This second FFT produces N Doppler filters, all of them for the pth range gate. This is repeated for all the range gates of interest. Fig. 10 points out that weight functions precede both levels of FFT.

The single correlator receiver was also simulated in software and applied to both P signals and LFM signals. The LFM signal was again simulated as phase coded signal with a quadratic phase low. In the simulation with LFM, K samples out of a total of M samples were used (taken at the centre of the sequence) to avoid the upper beat frequency. In the simulations with P signals, all the M samples were used, as there is only one beat frequency. This is another interesting property of P signals, discussed in Appendix 11.2.

The simulations revealed that with the single correlator receiver, both P signals and LFM signals yield the same response, and that response is similar to the theoretical response of LFM signals, drawn in Figs. 4 or 5. Thus, as far as LFM is concerned, there is no difference between the two types of receivers. As far as P signals are concerned, the low range sidelobes property is revealed only in the multicorrelator receiver.

9 Discussion and conclusions

Coherent processing of several periods of a periodically modulated CW signal was considered. A fourfold combination of two types of signals and two kinds of receivers was compared. The best sidelobe behaviour was reached when a P4 (or P3) signal was processed by a multicorrelator receiver (the equivalent of separate matched filters for all the elements of the delay-Doppler matrix). From the sidelobe level point of view, linear FM presented worse results, and these results did not differ much between the two types of receivers. The performances of P signals in the simple single correlator receiver were similar to those of LFM in that kind of receiver, and obviously worse than when the P signal was processed in a multicorrelator type receiver.

Since there is such a close relationship between P signals and LFM, why is this difference in range sidelobe performance, and would it disappear in the limit as M increases and t_b decreases. The answer to the later is negative. The low sidelobes of P signals are due to their special property of perfect periodic autocorrelation. This property is maintained for any M, as long as the phase sequence obeys the phase law given in eqn. 36 or eqn. 37.

There is a spectral penalty for the perfect periodic autocorrelation. As pointed out in Appendix 11.3, perfect periodic autocorrelation implies a 'sinc' type of spectrum, with its wide spectral sidelobes. Restricting the signal bandwidth will necessarily alter the ideal autocorrelation. This will introduce some range sidelobes, and some widening of the main lobe.

We emphasised range sidelobe levels because CW radars suffer most from nearby clutter, and low range sidelobes are critical in combating this problem (together with hardware requirements, such as linearity, over a wide dynamic range).

Another point for comparison is the issue of SNR loss. In the multicorrelator (matched filter) processor, the SNR loss is due to the weight function. As shown in Appendix 11.1, LFM suffers twice the loss (in dB) than P signal. With Hann weighting the loss is 1.76 dB for a P signal and 3.52 dB for an LFM signal. We have not analysed the SNR loss in the single correlator receiver, which departs from a matched filter by more than weights alone. We can only point out that LFM requires censoring of sections of each modulation period, to remove one of the two beat frequencies. This censoring entails SNR loss compared to the P signal which can process the entire sequence.

LFM has an advantage in having more degrees of freedom in the definition of the signal and the processor, than P signals. The high performances stressed in this discussion (in particular sidelobes), may rule out analog generation of the transmitted signal, where LFM could have had another advantage over P signals.

Towards the use of the preferred combination (P signal and multicorrelator receiver) we have pointed out an efficient multicorrelator processor, whose complexity is similar to the simple single correlator processor.

10 References

1 GRIFFITHS, H.D.: 'New ideas in FM radar', *Electron. Commun. Eng. J.*, 1990, **2**, (5), pp. 185–194
2 STOVE, A.G.: 'Linear FMCW radar techniques', *IEE Proc. F, Radar & Signal Process.*, 1992, **139**, pp. 343–350
3 FULLER, K.L.: 'To see and not be seen', *IEE Proc. F, Radar & Signal Process.*, 1990, **137**, pp. 1–9
4 KRETSCHMER, F.F., and LEWIS, B.L.: 'Doppler properties of polyphase coded pulse compression waveforms', *IEEE Trans. Aerosp. Electron. Syst.*, 1983, **AES-19**, pp. 521–531
5 BOMER, L., and ANTWEILER, M.: 'Binary and biphase sequences and arrays with low periodic autocorrelation sidelobes'. Proc. ICASSP-90, Albuquerque, NM, 1990, pp. 1663–1666
6 GOLOMB, S.W.: 'Two-valued sequences with perfect periodic autocorrelation', *IEEE Trans. Aerosp. Electron. Syst.*, 1992, **AES-28**, pp. 383–386
7 IPATOV, V.P., and FEDOROV, B.V.: 'Regular binary sequences with small losses in suppressing sidelobes', *Radioelectron. Commun. System.*, 1984, **27**, pp. 29–33
8 RIHACZEK, A.W.: 'Principles of high resolution radar' (McGraw-Hill, New York, 1969)
9 LEVANON, N., and FREEDMAN, A.: 'Periodic ambiguity function of CW signals with perfect periodic autocorrelation', *IEEE Trans. Aerosp. Electron. Syst.*, 1992, **AES-28**, pp. 387–395
10 NUTTALL, A.: 'Some windows with very good sidelobe behavior', *IEEE Trans. Acous., Speech, Signal Process.*, 1981, **ASSP-29**, pp. 84–91
11 CHU, D.C.: 'Polyphase codes with good periodic correlation properties', *IEEE Trans. Inf. Theor.*, 1972, **IT-18**, pp. 531–532
12 GRIFFITHS, H.D., and BRADFORD, W.J.: 'Digital generation of high time–bandwidth product linear FM waveforms for radar altimeters', *IEE Proc. F, Radar & Signal Process.*, 1992, **139**, pp. 160–169
13 HYMANS, A.J., and LAIT, J.: 'Analysis of a frequency-modulated continuous-wave ranging system', *IEE Proc. B*, 1960, **107B**, pp. 365–372

11 Appendix

11.1 SNR loss

The multicorrelator receiver differs from a matched receiver only by the weight function $w(t)$. Thus, the SNR loss, compared to the highest attainable SNR, is determined only by the weight function, as given by

$$\text{SNR loss} = \frac{[\int_0^{NT} w(t)\,dt]^2}{NT \int_0^{NT} w^2(t)\,dt} \tag{44}$$

The 2-term weight function used in a receiver matched to a P signal is (up to a constant)

$$w(t) = \left(1 - \frac{1-c}{c}\cos\frac{2\pi t}{NT}\right) \qquad 0 \leqslant t \leqslant NT \quad \text{zero elsewhere} \tag{45}$$

In the LFM case the weight function is

$$w(t) = \left(1 - \frac{1-c}{c}\cos\frac{2\pi t}{NT}\right)\left(1 - \frac{1-c}{c}\cos\frac{2\pi t}{T}\right)$$
$$0 \leqslant t \leqslant NT \quad \text{zero elsewhere} \tag{46}$$

Using eqns. 45 and 46 in eqn. 44 will yield

$$\text{SNR loss} = \begin{cases} \left[1 + \frac{1}{2}\left(\frac{1-c}{c}\right)^2\right]^{-1} & \text{P signal} \\ \left[1 + \frac{1}{2}\left(\frac{1-c}{c}\right)^2\right]^{-2} & \text{LFM} \end{cases} \tag{47}$$

With Hann weighting ($c = 0.5$) the loss is 1.76 dB for a P signal and 3.52 dB for LFM.

11.2 Beat frequency of P signals

A P3 signal with phase sequence as given in eqn. 37, will be used to demonstrate the existence of a single beat frequency. The same result would have been obtained with a P4 signal. If the phase sequence of the transmitted signal is according to a P3 sequence,

$$\phi(m) = \frac{\pi}{M}(m-1)^2 \quad m = 1, 2, \ldots, M \tag{48}$$

then the phase sequence of the received signal, delayed by k bits, is

$$\phi_k(m) = \begin{cases} \frac{\pi}{M}(M + m - k - 1)^2 & m \leqslant k \\ \frac{\pi}{M}(m - k - 1)^2 & m > k \end{cases} \tag{49}$$

The phase sequence of the beat signal will be the difference between the two sequences

$$\Delta\phi_k(m) = \phi(m) - \phi_k(m) \tag{50}$$

The effective beat frequency will be obtained from the difference between two consecutive phases of the beat signal

$$f_k(m) = \frac{1}{2\pi t_b}[\Delta\phi_k(m) - \Delta\phi_k(m-1)] \tag{51}$$

Using eqns. 49 and 50 in eqn. 51 we will get

$$t_b 2\pi f_k(m) = \begin{cases} \frac{2\pi k}{M} - 2\pi & m \leqslant k \\ \frac{2\pi k}{M} & m > k \end{cases} \tag{52}$$

Because of the modulo 2π property of phases, there is no difference between the two values, and we can rewrite eqn. 52 as

$$f_k(m) = \frac{k}{t_b M} \quad m = 1, 2, \ldots, M-1 \tag{53}$$

Thus we have shown that when a P3 sequence is multiplied by an identical but cyclic shifted sequence, the resulted beat signal has a single-value beat frequency along the entire sequence (independent of m). Its value is a function of the delay k. This is an interesting property of P3 and P4 signals which is not shared with LFM signals, except in the unique situation when the LFM receiver utilises a sampling interval which is exactly $t_s = 1/\Delta f$. In that particular case the two beat frequencies of LFM are folded one on top of the other. However, in many cases the sampling interval can be considerably longer than $1/\Delta f$.

11.3 Power spectral density

The power spectral density of LFM and P signals will be calculated through the Fourier transform of their autocorrelation $g_0(\tau)$. When the reference signal is the conjugate of the transmitted signal, $r(t) = u^*(t)$, the autocorrelation is given by $g_0(\tau)$. For LFM the autocorrelation is given in eqn. 24, while for P signals, as demonstrated by Fig. 6, one period of the autocorrelation can be described by

$$g_0(\tau) = \begin{cases} 1 - \frac{|\tau|}{t_b} & |\tau| \leqslant t_b \\ 0 & \text{elsewhere} \end{cases} \tag{54}$$

The power spectral density of a periodically modulated signal is constructed from spectral lines around the carrier frequency f_c and its negative image.

$$S(f) = \sum_{n=-\infty}^{\infty} |F_n| \delta\left[f \pm \left(f_c + \frac{n}{T}\right)\right]$$
$$n = 0, \pm 1, \pm 2, \ldots \tag{55}$$

where, when $r(t) = u^*(t)$,

$$F_n = \frac{1}{T}\int_{-T/2}^{T/2} g_0(\tau) \exp\left(-j2\pi n \frac{\tau}{T}\right) d\tau \tag{56}$$

Using eqn. 54 in eqn. 56 we get for the P signals

$$F_n = \frac{t_b}{T}\left(\frac{\sin(\pi n t_b/T)}{(\pi n t_b/T)}\right)^2 \tag{57}$$

For LFM we have to use eqn. 24 in eqn. 56, and solve numerically. The result for both signals appear in Fig. 11.

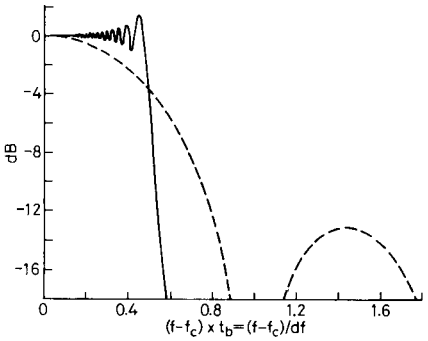

Fig. 11 *Half the power spectrum of LFM (solid) and P signals (dashed), when $t_b = 1/\Delta f$*

It was calculated using the relationship $t_b = 1/\Delta f$. Note the (first) spectral sidelobe of P signal, compared to the finite spectrum of LFM.